Magneto-caloric effect of a $Gd_{50}Co_{50}$ amorphous alloy near the freezing point of water

Cite as: AIP Advances **5**, 097122 (2015); https://doi.org/10.1063/1.4930832
Submitted: 27 May 2015 . Accepted: 27 August 2015 . Published Online: 08 September 2015

L. Xia, C. Wu, S. H. Chen, and K. C. Chan

Magneto-caloric effect of a $Gd_{50}Co_{50}$ amorphous alloy near the freezing point of water

L. Xia,[1] C. Wu,[1,2] S. H. Chen,[2] and K. C. Chan[2,a]
[1]*Laboratory for Microstructure, Institute of Materials, Shanghai University, Shanghai 200072, China*
[2]*Department of Industrial and Systems Engineering, The Hong Kong Polytechnic University, Hung Hom, Hong Kong*

(Received 27 May 2015; accepted 27 August 2015; published online 8 September 2015)

In the present work, we report the magneto-caloric effect (MCE) of a binary $Gd_{50}Co_{50}$ amorphous alloy near the freezing temperature of water. The Curie temperature of $Gd_{50}Co_{50}$ amorphous ribbons is about 267.5 K, which is very close to room temperature. The peak value of the magnetic entropy change ($-\Delta S_m^{peak}$) and the resulting adiabatic temperature rise ($\Delta T_{ad.}$) of the $Gd_{50}Co_{50}$ amorphous ribbons is much higher than that of any other amorphous alloys previously reported with a T_c near room temperature. On the other hand, although the $-\Delta S_m^{peak}$ of $Gd_{50}Co_{50}$ amorphous ribbons is not as high as those of crystalline alloys near room temperature, its refrigeration capacity (*RC*) is still much larger than the *RC* values of these crystalline alloys. The binary $Gd_{50}Co_{50}$ amorphous alloy provides a basic alloy for developing high performance multi-component amorphous alloys near room temperature. [http://dx.doi.org/10.1063/1.4930832]

I. INTRODUCTION

With the rising concerns on global warming and the ever increasing global consumption of energy in recent years, a number of new refrigeration technologies have been developed to replace the traditional vapor-cycle refrigeration in order to save energy and avoid ozone-depleting gases. Among these, magnetic refrigeration (MR) technology based on the magneto-caloric effect (MCE) of magnetic materials has shown promising application potential because it is regarded as a more energy efficient and environmentally friendly technique.[1–8] In MR technology, the working materials are critical and many magnetic materials with excellent MCE have been developed in the last few decades.[9–35]

Magneto-caloric materials can be divided into two types: materials that undergo a first-order magnetic phase transition, including most of the crystalline alloys such as Gd-Si-Ge, Ni-Mn-Ga, La-Fe-Si, Mn-As-Sb and Mn-Fe-P-As, and exhibit a sharp but narrow magnetic entropy change (ΔS_m) peak;[9–18] and materials that undergo a second-order magnetic phase transition, including amorphous alloys and a few crystalline alloys (for example, Gd and $Gd_6Co_2Si_3$), exhibit a broad distribution of the ΔS_m peak.[19–35] The amorphous alloys seem to be ideal candidates for magnetic refrigerants because they usually exhibit ultrahigh refrigeration capacity (*RC*, which is defined as the amount of heat that can be transferred in a thermodynamic cycle) due to their broadened magnetic entropy change *vs* temperature ($(-\Delta S_m)$-T) curve. In addition, they have a tunable Curie temperature (T_c) within a large compositional range, low energy loss due to their large electric resistance and ultralow magnetic hysteresis, better corrosion resistance and mechanical properties than their crystalline counterparts due to their unique disordered structures.[21–35]

However, the broadened $-\Delta S_m$ peaks of the amorphous alloys also induce a relatively low peak value of the magnetic entropy change ($-\Delta S_m^{peak}$) and a resultant low adiabatic temperature rise

[a]Corresponding author: Email: kc.chan@polyu.edu.hk

($\Delta T_{ad.}$) near T_c. Although recent efforts have demonstrated improved -ΔS_m^{peak} values comparable to pure Gd, and *RC* several times larger than crystalline alloys in some of the Gd-based bulk metallic glasses (BMGs), the T_c values of these BMGs are still much lower than room temperature.[27–35] On the other hand, some of the Fe-based amorphous alloys show a T_c near room temperature, but unfortunately, their -ΔS_m^{peak} is so low that they can hardly be applied as magnetic refrigerants.[21–24] Therefore, one of the key challenges for the application of amorphous alloys as magnetic refrigerants is to obtain large -ΔS_m^{peak} values near room temperature.

Our previous work on the glass forming ability (GFA) of a Gd-Co binary alloy system has shown that the $Gd_{50}Co_{50}$ is a better glass former in binary alloys and $Gd_{50}Co_{50}$ metallic glass can be fabricated in the shape of ribbons by melt-spinning.[36] In the present work, we studied the magnetic properties and magneto-caloric response of the $Gd_{50}Co_{50}$ amorphous alloy. The amorphous alloy shows excellent MCE with rather high -ΔS_m^{peak}, $\Delta T_{ad.}$ and *RC* values among the various amorphous alloys with T_c near room temperature.

II. EXPERIMENTS

A $Gd_{50}Co_{50}$ ingot was prepared by arc-melting 99.9% (at.%) pure Gd and Co under a titanium-gettered argon atmosphere. As-spun ribbons, about 40 μm in thickness, were prepared by a single copper wheel with a surface speed of about 30 m/s under a pure argon atmosphere. The structure of the ribbons was characterized by X-ray diffraction (XRD) on a Rigaku D\max-2550 diffractometer using Cu K_α radiation. The thermal properties of the ribbons were measured by Perkin-Elmer DIAMOND differential scanning calorimetry (DSC) under a purified argon atmosphere at a heating rate of 20 K/min. The magnetic properties of the $Gd_{50}Co_{50}$ amorphous ribbons were measured by a Quantum Design Physical Properties Measurement System (PPMS 6000). The temperature dependence of the magnetization (*M*-*T*) curve of the ribbons was measured from 150 K to 300 K under a field of 0.03 T. The hysteresis loops of the amorphous ribbons were measured under a field of 2 T at 150 K and 300 K respectively. The isothermal magnetization (*M*-*H*) curves of the ribbons were measured from 150 K to 320 K in steps of 5 K under a field of 5 T.

III. RESULTS AND DISCUSSION

Figure 1 shows the XRD pattern of the $Gd_{50}Co_{50}$ as-spun ribbons. The typical broad diffraction maxima in the XRD pattern of the as-spun ribbons indicate the features of the amorphous phases. The DSC trace of the $Gd_{50}Co_{50}$ as-spun ribbons is shown in the inset of Fig. 1. The glass transition followed by exothermic crystallization in the DSC trace also illustrates the amorphous feature of the as-spun ribbons.

Figure 2 shows the hysteresis loop of the $Gd_{50}Co_{50}$ as-spun ribbons measured at 150 K and room temperature under a field of 2 T. The amorphous ribbon is paramagnetic at room temperature,

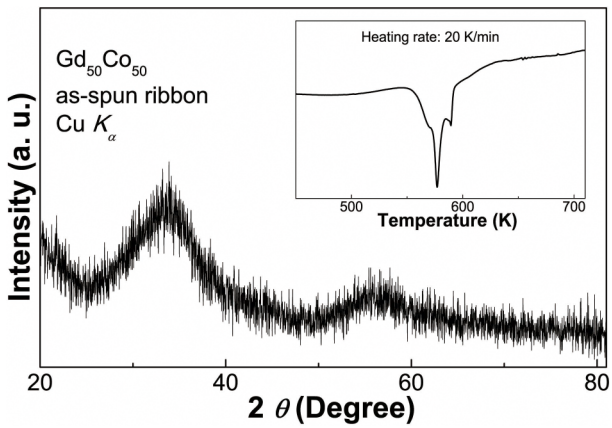

FIG. 1. XRD pattern of the $Gd_{50}Co_{50}$ as-spun ribbon, the inset is the DSC trance of the ribbon.

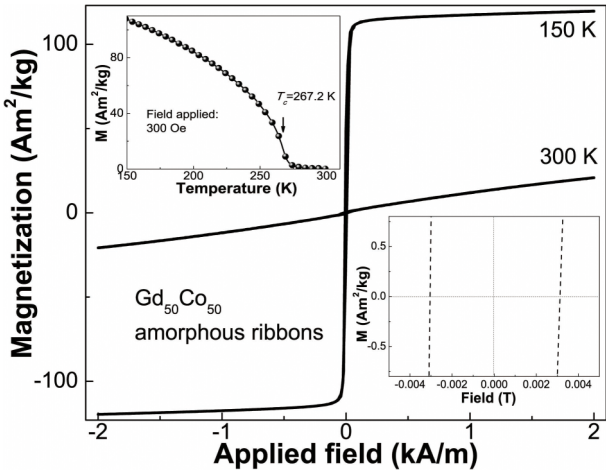

FIG. 2. Magnetic hysteresis loops of the $Gd_{50}Co_{50}$ as-spun ribbon at 150 K and 300 K under a magnetic field of 2 Tesla, the upper left inset shows the M-T curve of the amorphous ribbon under a field of 0.03 T and the lower right inset shows zoom of the hysteresis loop at low field.

and is soft magnetic at 150 K, with a saturation magnetization (M_s) of about 120 Am^2/kg and nearly zero coercivity (about 0.003 T, as shown in the lower right inset of Fig. 2). The M-T curve of the $Gd_{50}Co_{50}$ as-spun ribbons, measured from 150 K to 300 K under a field of 0.03 T, is shown in the upper left inset of Fig. 2. The Curie temperature (T_c) of the ribbons is about 267.2 K, which is very close to the freezing temperature of water, indicating that the amorphous alloy can be applied at sub-room temperature.

The temperature dependence of the magnetic entropy change ($(-\Delta S_m)$-T) curves for the $Gd_{50}Co_{50}$ amorphous ribbons can be derived from the isothermal magnetization (M-H) curves, according to the thermodynamic Maxwell equation

$$\Delta S_m(T,H) = S_m(T,H) - S_m(T,0) = \int_0^H \left(\frac{\partial M}{\partial T}\right)_H dH \tag{1}$$

Figure 3 shows the $(-\Delta S_m)$-T curves for the $Gd_{50}Co_{50}$ amorphous ribbons under different magnetic fields. The $-\Delta S_m^{peak}$ values of $Gd_{50}Co_{50}$ amorphous ribbons under fields of 1 T, 2 T, 3 T, 4 T and 5 T are listed in Table I. The $-\Delta S_m^{peak}$ values, under different magnetic fields, of other amorphous alloys, such as $Fe_{90}Zr_8B_2$ glassy ribbons at 240 K, $Fe_{88}Zr_8B_4$ glassy ribbons at 280 K, $Fe_{87}Zr_6B_6Cu_1$ amorphous ribbons at 300 K, $Fe_{86}Zr_7B_6Cu_1$ amorphous ribbons at 320 K,

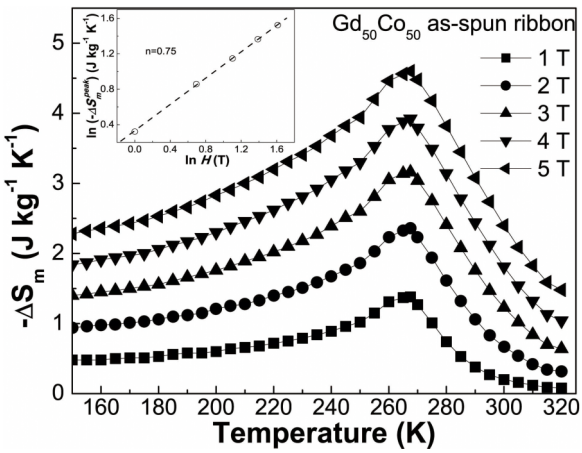

FIG. 3. $(-\Delta S_m)$-T curves of the $Gd_{50}Co_{50}$ as-spun ribbon under the field of 1 T, 2 T, 3 T, 4 T 5 T, the inset is the $\ln(-\Delta S_m^{peak})$ *vs* $\ln(H)$ plots for the ribbon.

TABLE I. The $-\Delta S_m^{peak}$ and *RC* under different magnetic fields of $Gd_{50}Co_{50}$ and other amorphous ribbons.

MCE of amorphous ribbons		1 T	2 T	3 T	4 T	5 T	Reference
$Gd_{50}Co_{50}$	$-\Delta S_m^{peak}$ ($Jkg^{-1}K^{-1}$)	1.38	2.36	3.16	3.92	4.6	Present work
	RC (Jkg^{-1})	89.6	212.8	366.9	506.9	685.9	
$Fe_{90}Zr_8B_2$	$-\Delta S_m^{peak}$ ($Jkg^{-1}K^{-1}$)	—	1.3	—	—	2.6	23
	RC (Jkg^{-1})	—	198	—	—	514	
$Fe_{88}Zr_8B_4$	$-\Delta S_m^{peak}$ ($Jkg^{-1}K^{-1}$)	—	1.3	—	—	2.8	23
	RC (Jkg^{-1})	—	201	—	—	551	
$Fe_{87}Zr_6B_6Cu_1$	$-\Delta S_m^{peak}$ ($Jkg^{-1}K^{-1}$)	—	1.6	—	—	3	23
	RC (Jkg^{-1})	—	208	—	—	590	
$Fe_{86}Zr_7B_6Cu_1$	$-\Delta S_m^{peak}$ ($Jkg^{-1}K^{-1}$)	—	1.6	—	—	3.1	23
	RC (Jkg^{-1})	—	205	—	—	582	
$Fe_{60}Cr_{14}Cu_1Nb_3Si_{13}B_9$	$-\Delta S_m^{peak}$ ($Jkg^{-1}K^{-1}$)	—	—	0.9	—	—	24
	RC (Jkg^{-1})	—	—	38	—	—	
$Fe_{76}Mo_4Cr_4Cu_1B_{15}$	$-\Delta S_m^{peak}$ ($Jkg^{-1}K^{-1}$)	1.07 under 1.5 T					22
	RC (Jkg^{-1})	82 under 1.5 T					
FeCoSiAlGaPCB	$-\Delta S_m^{peak}$ ($Jkg^{-1}K^{-1}$)	0.6 under 1.5 T					21
	RC (Jkg^{-1})	<10 under 1.5 T					

$Fe_{60}Cr_{14}Cu_1Nb_3Si_{13}B_9$ amorphous alloy at about 226 K, $Fe_{76}Mo_4Cr_4Cu_1B_{15}$ glassy ribbons at about 350 K and FeCoSiAlGaPCB amorphous alloy at about 320 K,[21–24] are also listed in Table I. Therefore, $Gd_{50}Co_{50}$ amorphous ribbons exhibit a rather high $-\Delta S_m^{peak}$ near room temperature compared with other amorphous alloys (the $-\Delta S_m^{peak}$ values for the $Fe_{76}Mo_4Cr_4Cu_1B_{15}$ and FeCoSiAlGaPCB amorphous ribbons obtained under 1.5 T are much lower than even the value of the $Gd_{50}Co_{50}$ amorphous ribbon under 1 T). On the other hand, another important parameter in evaluating the MCE for technical applications, the *RC* of the amorphous ribbon calculated by $RC = -\Delta S_m^{peak} \times \Delta T_m$ (where ΔT_m is the temperature range at the half maximum of the $-\Delta S_m^{peak}$), can also be obtained from the $(-\Delta S_m)$-*T* curves under different magnetic fields, as listed in Table I. The *RC* for the $Gd_{50}Co_{50}$ amorphous ribbons is also much higher than the values for the amorphous alloys mentioned above, and much larger than those of the intermetallic compounds with T_c near room temperature.[17,18]

The investigation on the field dependence of the magnetic entropy change may be helpful for better understanding the physical characteristics of amorphous materials.[34,35,37–39] In general, for soft magnetic amorphous alloys, the field dependence of the magnetic entropy change follows a $-\Delta S_m \propto H^n$ relationship: n=1 at a temperature well below T_c; in the paramagnetic range, n=2 as a consequence of the Curie-Weiss law; near T_c, n≈2/3 as proposed by Oesterreicher and Parker according to the mean field theory, or n≈0.72 as predicted by V. Franco and his co-workers according to the Arrott-Noakes equation. The $-\Delta S_m^{peak} \propto H^n$ fittings for the $Gd_{50}Co_{50}$ amorphous ribbons are shown in the inset of Fig. 3. The n value is found to be 0.75, which is similar to the values of other amorphous ribbons, indicating the similar magneto-caloric behavior and amorphous structure of these glassy ribbons. The n value obtained from the $-\Delta S_m^{peak}$-*H* curves is larger than the theoretical one predicted by the mean field theory and is believed to be due to the local inhomogeneities in the amorphous ribbons.

Although the $Gd_{50}Co_{50}$ amorphous ribbons show a $-\Delta S_m^{peak}$ larger than that of other amorphous alloys near room temperature, the value is still much lower than that of the Gd-based BMGs at low temperature.[25–35] Therefore, a more direct parameter, the adiabatic temperature rise, is employed for a comparison between different magneto-caloric materials under a particular magnetic field. The temperature dependence of $\Delta T_{ad.}$ ($\Delta T_{ad.}$-*T* curve) under a magnetic field can be obtained from the

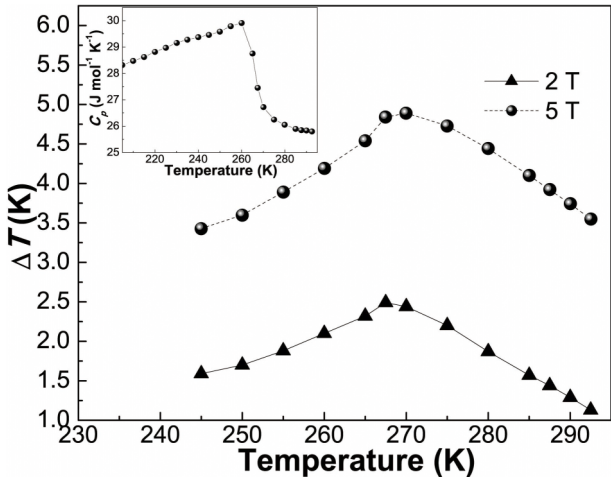

FIG. 4. The $\Delta T_{ad.}$-T curve of the $Gd_{50}Co_{50}$ as-spun ribbon under the field of 2 T and 5 T, the inset is the heat capacity of the $Gd_{50}Co_{50}$ amorphous ribbon under a zero magnetic field.

measured magnetization and the temperature dependence of the heat capacity ($C_p(T)$) as follows:

$$\Delta T_{ad}(T, 0 \rightarrow H) = -\frac{T}{C_p(T)} \Delta S_m(T, 0 \rightarrow H) \tag{2}$$

The temperature dependence of the heat capacity ($C_p(T)$) of the $Gd_{50}Co_{50}$ amorphous ribbons is shown in the inset of Fig. 4. Thus, combining the (-ΔS_m)-T curve and the $C_p(T)$ curve, we determine the ΔT_{ad}-T curve of the $Gd_{50}Co_{50}$ amorphous ribbons according to equation (2), as shown in Fig. 4. The peak value of the adiabatic temperature rise for the $Gd_{50}Co_{50}$ amorphous ribbons is about 4.9 K under 5 T and 2.4 K under 2 T, near 270 K, both of which are larger than most of the values of other amorphous alloys previously reported.[32–35]

It should be noted that the $Gd_{50}Co_{50}$ amorphous alloy is a binary alloy of simple composition. Thus, according to the empirical rules[40,41] and our previous work on the micro-alloying of BMGs, the GFA and MCE of the $Gd_{50}Co_{50}$ amorphous alloy can be further improved by alloying, doping and element substitution. Therefore, the $Gd_{50}Co_{50}$ amorphous alloy could be an ideal basic alloy for the development of high performance multi-component metallic glass, and it is envisaged that ternary or quarternary amorphous alloys with excellent MCE near room temperature will be fabricated in the near future.

IV. CONCLUSIONS

We report the magneto-caloric effect near room temperature of a $Gd_{50}Co_{50}$ amorphous alloy. The $Gd_{50}Co_{50}$ as-spun ribbons were fabricated by melt-spinning and their amorphous characteristics were demonstrated by the XRD and DSC. The Curie temperature is about 267.2 K and the saturation magnetization of the amorphous ribbon measured at 150 K under a field of 2 T is about 120 Am^2/kg. The -ΔS_m^{peak} and RC under different magnetic fields obtained from the isothermal magnetization curves of the $Gd_{50}Co_{50}$ amorphous ribbon are found to be higher than those of other amorphous alloys near room temperature, respectively. The field dependence of -ΔS_m^{peak} follows a -$\Delta S_m^{peak} \propto H^{0.75}$ relationship near the Curie temperature, indicating similar magneto-caloric behavior of the $Gd_{50}Co_{50}$ amorphous ribbon to that of other amorphous ribbons. The adiabatic temperature rise of the amorphous ribbon, approximately 4.9 K under 5 T and 2.4 K under 2 T near 270 K, is larger than most of the values of other amorphous alloys previously reported. All the above results indicate that amorphous $Gd_{50}Co_{50}$ is one of the best candidates for application as a magnetic refrigerant near the freezing temperature of water. The binary $Gd_{50}Co_{50}$ amorphous alloy constitutes an excellent basic alloy for developing multi-component amorphous alloys with enhanced GFA and MCE near room temperature.

ACKNOWLEDGEMENTS

The work described in this paper was supported by the Research Grants Council of the Hong Kong Special Administrative Region, China (Project No. PolyU 511212), the National Nature Science Foundation of China (Grant Nos. 51171100 and 51271103) and the MOST 973 (Grant No. 2015CB856800).

[1] V. K. Pecharsky and K. A. Gschneider, Jr., Phys. Rev. Lett. **78**, 4494 (1997).
[2] J. Glanz, Science **27**, 2045 (1998).
[3] V. K. Pecharsky and K. A. Gschneider, Jr., J. Magn. Magn. Mater. **200**, 44 (1999).
[4] O. Tegus, E. Brück, K. H. J. Buschow, and F. R. de Boer, Nature **415**, 150 (2002).
[5] A. M. Tishin and Y. I. Spichkin, *The Magnetocaloric Effect and Its Applications* (Institute of Physics Publishing Ltd. Bristol, 2003).
[6] E. Brück, J. Phys. D: Appl. Phys. **38**, R381 (2005).
[7] K. A. Gschneider, V. K. Pecharsky, and A. O. Tsokol, Rep. Prog. Phys. **68**, 1479 (2005).
[8] N. A. de Oliveira and P. J. von Ranke, Phys. Rep. **489**, 89 (2010).
[9] L. Morellon, J. Blasco, P. A. Algarabel, and M. R. Ibarra, Phys. Rev. B **62**, 1022 (2000).
[10] V. K. Pecharsky and K. A. Gschneider, Jr., Appl. Phys. Lett. **70**, 3299 (1997).
[11] F. X. Hu, B. G. Shen, J. R. Sun, and G. H. Wu, Phys. Rev. B. **64**, 132412 (2001).
[12] S. J. Kim, L. J. Lee, M. H. Jung, H. J. Oh, and Y. S. Kwon, J. Magn. Magn. Mater. **323**, 1094 (2011).
[13] A. Fujita, S. Fujieda, Y. Hasegawa, and K. Fukamichi, Phys. Rev. B **67**, 104416 (2003).
[14] O. Tegus, E. Brück, K. H. J. Buschow, and F. R. de Boer, Nature **415**, 150 (2002).
[15] H. Wada and Y. Tanabe, Appl. Phys. Lett. **79**, 3302 (2001).
[16] L. G. de Medeiros, Jr. and N.A. de Oliveira, J. Alloys Compd. **501**, 177 (2010).
[17] M. H. Phan and S. C. Yu, J. Magn. Magn. Mater. **308**, 325 (2007).
[18] V. Provenzano, A. J. Shapiro, and R. D. Shull, Nature (London) **429**, 853 (2004).
[19] G. V. Brown, J. Appl. Phys. **47**, 3673 (1976).
[20] J. Sun, J. F Wu, and J. R. Sun, J. Appl. Phys. **106**, 083902 (2009).
[21] V. Franco, J. M. Borrego, A. Conde, and S. Roth, Appl. Phys. Lett. **88**, 132509 (2006).
[22] V. Franco, C. F. Conde, A. Conde, and L. F. Kiss, Appl. Phys. Lett. **90**, 052509 (2007).
[23] P. Alvarez-Alonso, J. L. Sánchez Llamazares, C. F. Sánchez-Valdés, M. L. Fdez-Gubieda, P. Gorria, and J. A. Blanco, J. Appl. Phys. **117**, 17A710 (2015).
[24] S. Atalay, H. Gencer, and V. S. Kolat, J. Non-Cryst. Solids **351**, 2373 (2005).
[25] Q. Luo, D. Q. Zhao, M. X. Pan, and W. H. Wang, Appl. Phys. Lett. **92**, 011923 (2008).
[26] L. Liang, X. Hui, Y. Wu, and G. L. Chen, J. Alloys Compds. **457**, 541 (2008).
[27] Q. Luo, D. Q. Zhao, M. X. Pan, and W. H. Wang, Appl. Phys. Lett. **89**, 081914 (2006).
[28] J. Du, Q. Zheng, Y. B. Li, Q. Zhang, D. Li, and Z. D. Zhang, J. Appl. Phys. **103**, 023918 (2008).
[29] L. Xia, K. C. Chan, and M. B. Tang, J. Alloys Compd. **509**, 6640 (2011).
[30] S. Lu, M. B. Tang, and L. Xia, Physica B **406**, 3398 (2011).
[31] N. S. Bingham, H. Wang, F. Qin, H. X. Peng, J. F. Sun, V. Franco, H. Srikanth, and M. H. Phan, Appl. Phys. Lett. **101**, 102407 (2012).
[32] P. Wang, K. C. Chan, S. Lu, M. B. Tang, and L. Xia, Chin. Phys. Lett. **29**, 096103 (2012).
[33] F. Yuan, J. Du, and B. Shen, Appl. Phys. Lett. **101**, 032405 (2012).
[34] L. Xia, K. C. Chan, M. B. Tang, and Y. D. Dong, J. Appl. Phys. **115**, 223904 (2014).
[35] L. Xia, Q. Guan, D. Ding, M. B. Tang, and Y. D. Dong, Appl. Phys. Lett. **105**, 192402 (2014).
[36] Y. F. Ma, P. Yu, and L. Xia, Mater. Design **85**, 715 (2015).
[37] H. Oesterreicher and F. T. Parker, J. Appl. Phys. **55**, 4336 (1984).
[38] V. Franco, J. M. Borrego, C. F. Conde, A. Conde, M. Stoica, and S. Roth, J. Appl. Phys. **100**, 083903 (2006).
[39] V. Franco, J. S. Blázquez, and A. Conde, J. Appl. Phys. **100**, 064307 (2006).
[40] A. Inoue, T. Zhang, and A. Takeuchi, Mater. Sci. Forum **269**, 855 (1998).
[41] W. L. Johnson, MRS Bulletin **24**, 42 (1999).